Strength and equation of state of boron suboxide from radial x-ray diffraction in a diamond cell under nonhydrostatic compression

Duanwei He,* Sean R. Shieh,† and Thomas S. Duffy
Department of Geosciences, Princeton University, New Jersey 08544, USA
(Received 28 May 2004; published 23 November 2004)

Using radial x-ray diffraction techniques together with lattice strain theory, the behavior of boron suboxide (B_6O) was investigated under nonhydrostatic compression to 65.3 GPa in a diamond-anvil cell. The apparent bulk modulus derived from nonhydrostatic compression data varies from 363 GPa to 124 GPa depending on the orientation of the diffraction planes with respect to the loading axis. Measurement of the variation of lattice spacing with angle, ψ, from the loading axis allows the d spacings corresponding to hydrostatic compression to be obtained. The hydrostatic d spacing obtained from a linear fitting to data at 0° and 90° is consistent with direct measurements at the appropriate angle ($\psi=54.7°$) to within 0.5%, which suggests that even two measurements ($\psi=0°$ and 90°) are sufficient for accurate hydrostatic equation of state determination. The hydrostatic compression data yield a bulk modulus $K_0=270\pm12$ GPa and its pressure derivative $K_0'=1.8\pm0.3$. The ratio of differential stress to shear modulus ranges from 0.021 to 0.095 at pressures of 9.3–65.3 GPa. Together with estimates of the high-pressure shear modulus, a lower bound to the yield strength is 26–30 GPa at the highest pressure. The yield strength of B_6O is about a factor of 2 larger than for other strong solids such as Al_2O_3. The ratio of yield stress to shear modulus derived from lattice strain theory is also consistent with the result obtained by the analysis of x-ray peak width. This ratio might be a good qualitative indicator of hardness as it reflects the contributions of both plastic and elastic deformation.

DOI: 10.1103/PhysRevB.70.184121 PACS number(s): 62.50.+p, 62.20.Dc, 64.30.+t

INTRODUCTION

Boron compounds have generated considerable interest as strong solids.[1–10] Recently, boron suboxide (B_6O) was found to be as hard as cubic boron nitride and have a fracture toughness similar to that of diamond.[1] It combines extreme hardness, high chemical inertness, low mass density, high thermal conductivity, and excellent wear resistance.[1–5] Moreover, boron suboxide can be synthesized at much lower pressure (even at ambient pressure[6–10]) compared to diamond and cubic boron nitride. This significantly adds to the commercial attractiveness of boron suboxide as a superhard material.

Despite great potential applications as a superhard material, direct experimental measurements of elastic properties, strength, and plastic deformation behavior of boron suboxide at high pressures are limited. To date, the only experimental measurement of elastic moduli for crystalline boron suboxide was reported by Petrak *et al.* in 1974.[11] They obtained the aggregate elastic moduli for near-zero porosity (<1%) hot-pressed boron suboxide specimens at ambient conditions using the resonant-sphere technique. The bulk modulus (K), shear modulus (G), and Young's modulus (Y) were determined to be 230 GPa, 206 GPa, and 472 GPa, respectively. However, the elastic properties of the hot-pressed sample may be related to the sintering conditions, and boron suboxide materials synthesized at low pressure are generally oxygen deficient (B_6O_x, $x<0.9$) with poor crystallinity,[1,7,10] which may also affect the measured elastic moduli. *Ab initio* calculations gave a value of 222 GPa for the bulk modulus of boron suboxide,[2] which is close to the experimental data of Petrak *et al.* More recently, Music *et al.*[12] determined Young's modulus for amorphous boron suboxide using classical molecular dynamics (MD) simulations as well as elastic recoil detection analysis based on nanoindentation measurements of the thin films. Their results gave values of 231–273 GPa from experimental measurements, and 196–275 GPa from the MD simulation depending on oxygen incorporation. According to the above data, it appears that the elastic moduli of boron suboxide are far lower than those of the cubic boron nitride ($K=400$ GPa, $G=409$ GPa, $Y=973$ GPa).[13–15] Although there is a certain correlation between the elastic moduli and the hardness values for some classes of material,[13–15] the dependence is not monotonic as both elastic and plastic deformations are generally involved in the hardness testing process. Therefore, it is interesting to look at the elastic moduli of well-crystallized boron suboxides with high oxygen occupancy using different techniques and investigate its plastic deformation behavior under high stress.

High-pressure experiments using diamond-anvil cells combined with synchrotron x-ray diffraction are one of the best means to obtain fundamental information on the equation of state of materials over large ranges of compression. From an experimental point of view, high-pressure studies on B_6O are challenging because of the low atomic number of both boron and oxygen, which leads to weak x-ray diffraction signals given the small sample volumes in a diamond-anvil cell. This is probably the reason that although boron suboxide was first synthesized by Weintraub in 1909 (Ref. 9) no experimental data on its equation of state (EOS) has been reported. A sample in the gasketed diamond-anvil cell is always subjected to a uniaxial stress at high pressure. Even if the sample is initially contained within a fluid pressure medium, a completely hydrostatic environment cannot be sustained above ~15 GPa due to the freezing of all known pressure media at room temperature.[16] The presence of

nonhydrostatic stress is known to bias equation of state determination, especially for strong materials.[17,18] For example, the bulk modulus of rhenium derived from nonhydrostatic compression data can vary nearly a factor of 2 depending on the relative orientation of the diffraction vector and the diamond cell stress axis.[18] For boron suboxide, the nonhydrostaticity may even have a stronger effect on the equation of state parameters. Recently developed radial x-ray diffraction techniques[17–22] make it possible to obtain a hydrostatic compression curve from the highly nonhydrostatic data by proper choice of the orientation between the stress axis and diffraction vector. Those techniques have been applied for hydrostatic EOS determination of Re, Mo, SiO_2, and $CaSiO_3$, and the results were in agreement with other quasihydrostatic measurements.[17,18,22,23] The radial diffraction technique holds much promise from equation of state determination at very high pressures (>40 GPa), where it becomes increasingly difficult to maintain a quasihydrostatic environment through the use of soft-pressure transmitting media.

In this study, we examine the behavior of boron suboxide in the diamond-anvil cell under nonhydrostatic compression. Using radial x-ray diffraction technique together with the lattice strain theory[19–21] enables us to observe the strain at any orientation relative to the loading axis, to constrain the hydrostatic compression curve under nonhydrostatic compression, and to obtain the information related to both elastic and plastic properties of the boron suboxide sample.

EXPERIMENT

Boron suboxide was synthesized in a belt-type large volume press at 5.5 GPa and 1900 °C for 60 min starting from a mixture of crystalline boron and amorphous boron oxide (B_2O_3).[10] The orange-red crystalline sample powder has a average grain size of ~4 μm with a euhedral morphology. The cell volume was determined to be 311.5 Å^3 from powder x-ray diffraction at ambient conditions. The composition was estimated to be $B_6O_{0.98}$ by electron energy loss spectroscopy measurements. The structure of boron suboxide is built of eight icosahedra at the apices of the rhombohedral unit cell (space group $R\bar{3}m$).[7] Each icosahedron is composed of 12 boron atoms. Two oxygen atoms are located in the interstices along the [111] rhombohedral direction.

The boron suboxide sample was loaded into a 90-μm diameter hole of a Be gasket. The gasket was preindented to ~25 μm thickness at ~20 GPa. A piece of ~15-μm Au foil was placed on top within 5 μm of the sample center. Special attention was paid to make sure that sample hole was well centered with respect to the anvil culet. The gold foil served as a pressure standard[24] as well as a position reference for x-ray diffraction.[17,18] We used a symmetric diamond-anvil cell to exert nonhydrostatic compression on both the B_6O sample and Au. No pressure-transmitting medium was used. Energy-dispersive radial x-ray diffraction experiments[17–19] were performed at the X17C beam line of the National Synchrotron Light Source at Brookhaven National Laboratory. The incident x-ray beam was focused by a pair of Kirkpatrick-Baez mirrors to approximately 10×15 μm and directed through the Be gasket and the sample. The diffracted intensity was detected by a solid-state Ge detector with a fixed angle at $2\theta=7.991(3)°$, which was calibrated with a separate gold foil. Two collimators are located along the scattered beam path. The front collimator, located ~6.5 cm from the sample with an opening of 30 μm, provides spatial filtering while the rear collimator defines the scattering angle. A significant advantage of the use of the energy-dispersive method for radial-geometry diffraction is that the capability of spatial filtering reduces the strong background that can arise from the gasket while also ensuring that the diffracted intensity is restricted to the region near the loading axis of the cell.

The diamond-anvil cell was mounted in a rotation stage whose axis bisects 2θ. Thus the angle, ψ, between the diffraction plane normal and the cell-loading axis could vary from 0° (diffraction normal parallel to the diamond cell loading axis) to 90° (diffraction normal perpendicular to loading axis). Before data collection, the cell was scanned in the horizontal and vertical direction while recording x-ray transmission with a photodiode. The strong absorption due to the gold foil was readily detectable, and thus we ensure that the Au foil was always centered within the x-ray beam to ±5 μm. However, as the size of the Au is small (15–20 μm upon compression), and there is no obvious contrast in the x-ray scans between the Be gasket and B_6O sample, locating the Au after cell rotation or pressure increase could be time-consuming. Diffraction spectra were collected only after sufficient time (more than 1 h) elapsed after each compression step to allow for stress relaxation. A total of 9 pressure steps were investigated. Except for the first two steps, diffraction patterns were taken at $\psi=0°$, 90°, 54.7°, respectively. At higher pressures, we always rotated the stage back to $\psi=0°$ and collected data again to compare with the patterns taken at the beginning. The data collecting time was 30–60 min for a single spectrum. The variation in d spacing at $\psi=0°$ was typically less than 0.3% over the measurement time interval and not systematic (i.e., the d spacing obtained from the last pattern was not always larger or less than that from the first one at a given loading step). For comparison, the change in d spacing from $\psi=0°$ to 90° is ~5% at the highest pressure. At the final loading step, diffraction patterns were also collected along a linear transect across the sample surface at 20 μm steps at $\psi=0°$. The change in d spacing of boron suboxide within 20 μm was found to be less than 0.8%. The effect of position change on Au lattice parameters was not detectable. With the diamond cell oriented at $\psi=0°$, we also carried out a transect along the loading axis (at right angles to the diamond surface) and found no detectable change in the diffraction peak positions for Au or boron suboxide with distance from the diamond surface.

Peak positions were obtained by fitting background subtracted Voigt line shapes to the spectra. The lattice parameters of Au were derived from the diffraction lines of (111), (200), and (220). The Au (311) line was also available below 20 GPa. Hydrostatic pressures were obtained from the mean lattice parameter of gold at $\psi=54.7°$. As reported previously,[18,22] the (200) diffraction line of gold is anomalous. This may be a consequence of plastic deformation.[25,26] However, the effect of including or excluding (200) on pressure determination was small (<1 GPa). For boron subox-

TABLE I. Observed *d* spacing of boron suboxide (104), (012), and (003) planes at different pressures and angles.

	d spacing (Å)								
	(104)			(012)			(003)		
P (GPa)	90°	54.7°	0°	90°	54.7°	0°	90°	54.7°	0°
1.5(0.2)			2.5748			3.7302			4.0882
9.3(0.5)	2.5523		2.5211	3.7096		3.6707	4.0765		4.3098
18.3(0.4)	2.5220	2.5148	2.4651	3.6729	3.6469	3.5659	4.0299	4.0016	3.9580
			2.4642			3.5750			3.9607
26.8(0.6)	2.4930	2.4840	2.4305	3.6409	3.6071	3.5241	3.9890	3.9469	3.9051
			2.4228			3.4983			3.8882
43.5(0.7)	2.4668	2.4373	2.3796	3.5987	3.5502	3.4338	3.9366	3.8748	3.7854
			2.3715			3.4480			3.7719
50.6(0.9)	2.4474	2.4180	2.3502	3.5774	3.5257	3.3989	3.9000	3.8396	3.7309
			2.3513			3.3959			3.7411
59.8(0.6)	2.4331	2.3980	2.3350	3.5726	3.5015	3.3814	3.8743	3.8116	3.6931
			2.3320			3.3777			3.7411
65.3(0.9)	2.4200	2.3906	2.3251	3.5307	3.4771	3.3437	3.8294	3.7772	3.6599
			2.3199			3.3513			3.6570
			2.3076			3.3431			3.6446

ide, the diffraction lines (101), (003), (012), (110), (104), and (021) could be detected. In some cases, the (021) line of B_6O was overlapped by Au (111), and the (101) and (110) lines were not used due to their very low intensity. However, the (003), (012), and (104) lines of B_6O were observable through the entire range of our measurements. The lattice parameters of boron suboxide were generally derived from diffraction lines of (003), (012), and (104) using least-squares fitting to a hexagonal cell. Table I lists the observed *d* spacings of the (003), (012), and (104) planes of boron suboxide at $\psi=0°$, 90°, 54.7° at different pressures, and representative diffraction spectra are shown in Fig. 1.

THEORY

The radial x-ray diffraction data was analyzed using the lattice strain theory developed by Singh and co-workers.[19–21] According to this theory, the stress state in a polycrystalline sample under nonhydrostatic compression in the diamond-anvil cell can be described by a maximum stress along the cell loading axis, σ_3, and a minimum stress in the radial direction, σ_1. The difference between σ_3 and σ_1 is the uniaxial stress component *t*,

$$t = \sigma_3 - \sigma_1 \leqslant 2\tau = Y, \tag{1}$$

where τ is the shear strength and *Y* the yield strength of the sample. The equality in relation (1) holds for a von Mises yield condition and *t* could be less than the yield strength.

The observed *d* spacing (d_m) is a function of the angle ψ between the diamond cell loading axis and diffraction plane normal:

$$d_m(hkl) = d_p(hkl)[1 + (1 - 3\cos^2\psi)Q(hkl)], \tag{2}$$

where $d_p(hkl)$ is the *d* spacing resulting from the hydrostatic component of stress, and

$$Q(hkl) = (t/3)\{\alpha[2G_R(hkl)]^{-1} + (1-\alpha)(2G_V)^{-1}\}. \tag{3}$$

$G_R(hkl)$ is the aggregate shear modulus of grains contributing to the diffraction intensity under the condition of constant stress across grain boundaries (Reuss limit). G_V is the shear modulus under isostrain conditions (Voigt bound). The parameter α ranges from 1 to 0 depending on the degree of

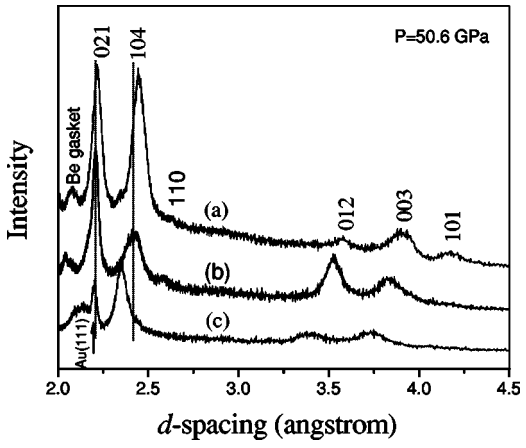

FIG. 1. XRD patterns of the sample taken at $\psi=0°$ [curve (c)], 54.7° [curve (b)], and 90° [curve (a)] under the same loading. The position of B_6O (104) and Au (111) diffraction peaks at $\psi=54.7°$ are marked by a solid line for comparison. B_6O (021) peaks are overlapped by Au (111) on curves (a) and (b).

stress and strain continuity across grains in the polycrystalline sample.

According to Eq. (2), $d_m(hkl)$ should vary linearly with $1-3\cos^2\psi$. It reaches a maximum at $\psi=90°$ and minimum at $\Psi=0°$. At $\psi=54.7°$ $(1-3\cos^2\psi=0)$, the position of the observed x-ray diffraction line reflects the d spacing due to the hydrostatic component of stress, and there is no contribution to the measured d spacing from the differential stress. Local deviatoric stresses will also exist producing grain to grain strain differences, but these result in broadening of the diffraction lines rather than peak shift.[19]

The aggregate polycrystalline sample in the diamond-anvil cell is generally assumed to be under isostress conditions (Reuss limit). In this case, α equals 1 in Eq. (3) and the uniaxial stress component can be expressed as

$$t = 6G\langle Q(hkl)\rangle, \tag{4}$$

where $\langle Q(hkl)\rangle$ presents the average $Q(hkl)$ value over all observed reflections, and G is the aggregate shear modulus of the polycrystalline sample. If the uniaxial stress t has reached its limiting value of yield strength at high pressures, $6\langle Q(hkl)\rangle = t/G$ will reflect the ratio of yield strength to shear modulus. According to Eq. (2), the slope of the $d_m(hkl)$ vs $1-3\cos^2\psi$ relation yields the product $d_p(hkl)Q(hkl)$, and $d_p(hkl)$ can directly be measured at $\psi=54.7°$.

RESULTS AND DISCUSSION

Diffraction spectra of the sample were measured to conditions corresponding to a hydrostatic pressure up to 65.3 GPa at room temperature. At the each loading, it was found that diffraction peaks always shifted to smaller d spacing as ψ decreased, reflecting that increase in strain as the diffraction plane normal approaches the maximum stress axis. This can be clearly seen in Fig. 1, which shows the patterns taken at $\psi=90°$, 54.7°, and 0° at 50.6 GPa. Here the pressure is determined using the Au scale[24] from the diffraction data obtained at $\psi=54.7°$. At room temperature, there are some differences in the reported equations of state for Au. The recent EOS of Au by Shim *et al.*[24] yields a ~3 GPa pressure difference from that of Anderson *et al.*[27] at 60 GPa and room temperature. The shift of diffraction lines for B_6O is larger than that for Au. This indicates that B_6O is stronger than Au and can support a larger uniaxial stress. To further demonstrate the above phenomenon, we plotted the apparent relative volume change (V/V_0) of B_6O and Au at $\psi=90°$, 54.7°, and 0° as a function of pressure in Fig. 2. The difference of the observed V/V_0 between 90° (minimum stress direction) and 0° (maximum stress direction) under the same loading for boron suboxide is far larger than that for gold, and both tend to increase with pressure. The change of the observed V/V_0 with direction is caused by the uniaxial stress field. The difference of the measured V/V_0 between 90° and 0° is related to the uniaxial stress component $t=\sigma_3-\sigma_1$, which is limited by the yield strength of the material. Gold has a low yield strength, and the uniaxial stress it can support is less than 1 GPa under nonhydrostatic compression to 50 GPa in a diamond cell.[18,22] But strong metals such as Mo and Re are found to support a deviatoric stress of ~7 GPa at the same condition.[18,22] As a potential superhard material, we expect that boron suboxide could support even a higher uniaxial stress.

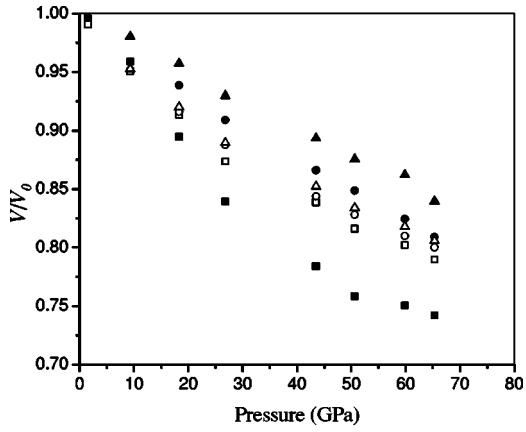

FIG. 2. Observed apparent V/V_0 of B_6O (solid symbols) and Au (open symbols) at $\psi=0°$ (squares), 54.7° (circles), and 90° (triangles) under different pressures. The pressure is determined from the mean lattice parameter of gold obtained at $\psi=54.7°$.

For the conventional axial experiments using the diamond-anvil cell, *in situ* x-ray diffraction measurements are confined to near the minimum strain direction. Thus the observed lattice strain is smaller than the strain component due to the hydrostatic pressure. But the measured value is closer to the hydrostatic strain if the material has a lower strength. In this case, the nonhydrostatic compression curve will yield a volume that lies above the quasihydrostatic curve at a given pressure when the pressure standard material is weaker than the studied material or when a fluorescence standard such as ruby is used.[18] But if the pressure standard material is stronger than the studied material, the nonhydrostatic compression curve observed will lie below the quasihystatic curve in the P-V plane. In other words, the strength difference between the studied material and pressure standard material determines how the observed compression curve biases the quasihydrostatic curve.

Figure 3 shows plots of d spacing as a function of $1-3\cos^2\psi$ for selected diffraction lines of gold and boron suboxide at six different pressures. As expected from the theory, our measured d spacings vary linearly with $1-3\cos^2\psi$. The diffraction peaks of boron suboxide exhibits a slope that is about 10 times as great as that of gold peaks at the highest pressure, which again indicates that boron suboxide is more sensitive to nonhydrostatic stresses. The d spacing at $\psi=54.7°$ (d_{hydro}) could be estimated from the corresponding observed values at $\psi=0°$ (d_0) and 90° (d_{90}):

$$d_{hydro} \approx (d_0 + 2d_{90})/3. \tag{5}$$

The relative error of the calculated d_{hydro} from Eq. (5) was less than 0.5%. If a linear relation [Eq. (2)] holds, then the d spacing from different ψ angle can be determined if we have at least two d spacings from different ψ at a given loading. In contrast to previous radial diffraction studies, we collected diffraction patterns at only three angles at each loading step.

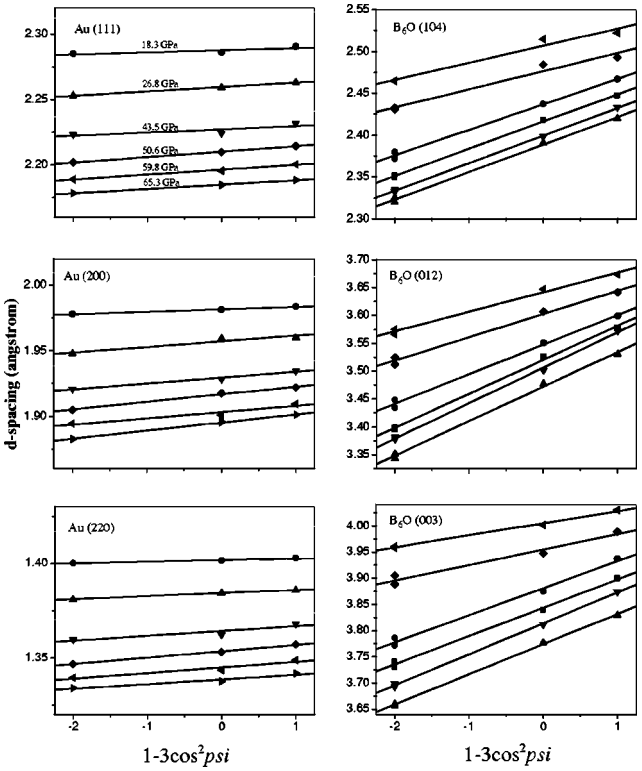

FIG. 3. Dependence of observed d spacing on $1-3\cos^2\psi$ for selected diffraction lines of gold and boron suboxide at different pressures. The two data points of boron suboxide for each pressure step at $1-3\cos^2\psi=-2$ ($\psi=0°$) were obtained at the beginning and end of the measurements. The solid lines are least-squares fits to the data. The pressures are determined from mean lattice parameter of Au at $\psi=54.7°$.

For energy dispersive diffraction, this maximizes the number of pressure steps that can be carried out using weakly scattering samples. The good agreement between d_{hydro} and our measurements at $\psi=54.7°$ shows that even two measurements ($\psi=0°$ and 90°) are sufficient for accurate hydrostatic equation of state determination.

Using the equation of state of gold,[24] the hydrostatic pressure was determined from the mean lattice parameter at $\psi=54.7°$ for each loading step. The compression curves for boron suboxide at 90°, 54.7°, and 0° are shown in Fig. 4. It was found that the c/a ratio of the boron suboxide hexagonal unit cell slightly decreased from 2.275 to 2.232 as the pressure increased to 65.3 GPa from 1.5 GPa without dependence on the angle ψ. The unit-cell volumes observed at different pressures were fitted to the third-order Birch-Murnaghan equation of state. At $\psi=54.7°$, we obtained the bulk modulus $K_0=270\pm12$ GPa and its pressure derivative $K_0'=1.8\pm0.3$. With K_0' fixed at 4, the derived K_0 is 213 ± 57 GPa, which has a relative large standard error but is close to the data of Petrak *et al.*[11] and the value from *ab initio* calculations.[2] Our pressure derivative of 1.8 ± 0.3 is lower than usual values, which are typically around 4. However, pressure derivates of 3 or lower have been reported previously for incompressible solids such as cubic boron nitride and diamond.[28–31] The bulk moduli obtained from fits of the diffraction data at 0° and 90° are 363 GPa and

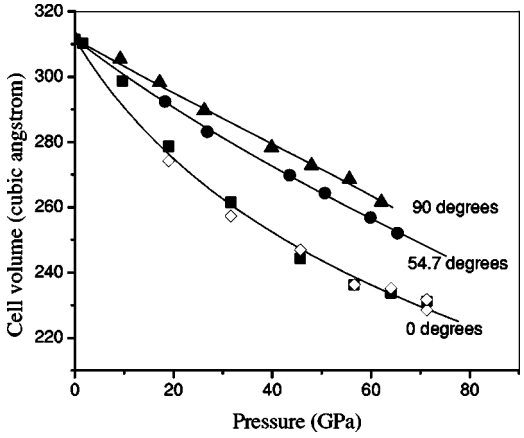

FIG. 4. Compression curves of boron suboxide from lattice parameters measured at 0°, 54.7°, and 90°. The pressure is also calculated from the measured diffraction data of gold at 0°, 54.7°, and 90°. The solid lines are Birch-Murnaghan equation fits to the data at $\psi=0°$, 54.7°, and 90°. The solid squares and open diamonds are the cell volume observed at the beginning and end of the measurements for the same loading step at $\psi=0°$.

124 GPa, respectively. Thus for a superhard material such as boron suboxide, the bulk modulus derived from the nonhydrostatic compression data can vary nearly a factor of 3 depending on the relative orientation of the diffraction vector and diamond cell stress axis. This is also consistent with the data reported by Duffy *et al.*,[18,22] in which a total variation of 65% and 94% for the bulk modulus of molybdenum and rhenium was observed using the gold pressure scale. The above results again illustrate that the nonhydrostaticity can have a stronger effect on equation of state parameters, particularly for strong imcompressible solids.

According to our measurements and the reported data, the bulk modulus of the boron suboxide is only ~65% of that for cubic boron nitride, though they have a similar Vickers hardness.[1] Various elastic moduli are frequently used as an indicator to search for new superhard materials in theoretical calculations.[13–15,32] Therefore, it is interesting to critically look at the correlation between the elastic moduli and hardness. There are many definitions of hardness, as there are many ways of testing it. In a general sense, hardness is the resistance to external mechanical action to scratch, abrade, indent, or any other way permanently affect its surface.[13,33] Those tests tend to measure the deformation of the material under a external shear, which is initially elastic, but in later stage displays yield. Thus hardness must be related to both the elastic and plastic properties of a material. In the initial elastic deformation stage, the material, which has a high hardness, should have a high bulk modulus to resist the volume decrease under the applied pressure, as well as a high shear modulus to prevent the deformation in a direction different from the applied load. Although there is a certain correlation between the bulk modulus and the hardness for particular classes of substance, the shear modulus was found to be a significantly better qualitative predictor of hardness.[13–15] However, the later plastic deformation stage of hardness measurement is not controlled by the shear modulus but by the shear strength, which can vary by more than a factor of

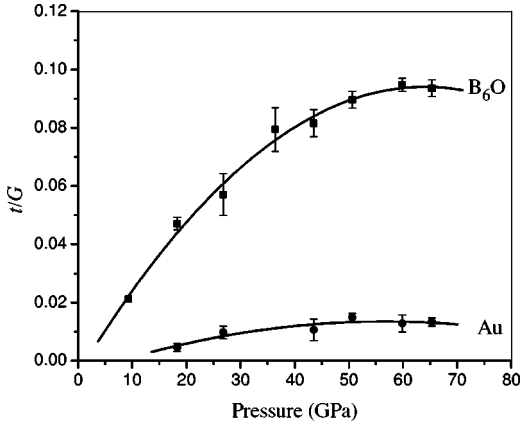

FIG. 5. Ratio of differential stress to shear modulus (t/G) as a function of pressure for boron suboxide and gold. The solid lines are polynomial fits to the data. The pressures are determined from the mean lattice parameter of gold obtained at $\psi=54.7°$. The estimated errors are obtained from the scatter of $d(hkl)$ vs $1-3\cos^2\psi$.

10 for different materials with similar shear modulus.[14,34] The ratio of shear strength, τ, to shear modulus, G, could be more useful as it reflects the contributions of both plastic and elastic deformation. In fact, the theoretical studies of ideal strength of solids are typically expressed in terms of τ/G, which is of the order of 0.03–0.04 for a face-centered-cubic metal, 0.15 for an ionic compound such as sodium choride, and 0.25 for a purely covalent material such as diamond.[14,34]

The ratio of differential stress to shear modulus (t/G) was plotted as a function of pressure for gold and boron suboxide in Fig. 5. The t/G obtained for gold in this study agrees well with the previous reported data.[18,22] For example, both our measurements and the reported data in Refs. 13 and 24 give a value of ~0.01 for t/G of gold at ~40 GPa. For boron suboxide, the t/G ranges from 0.021 to 0.095 and increases with pressure. But the increase in t/G levels off after ~50 GPa. Similar behavior was observed for cubic silicon nitride (c-Si_3N_4),[35] which is also a superhard material with a reported Vickers hardness of 43 GPa.[36] The change of t/G with pressure may indicate that the boron suboxide started to yield and t reaches its limiting value of Y (yield strength) at a nonhydrostatic compression of ~40–50 GPa. It is interesting that this pressure also corresponds to a relative intensity change of the diffraction peaks. Figure 6 shows the selected diffraction patterns of the sample taken at $\psi=54.7°$ under different pressures. The change in relative intensity of the boron suboxide peaks was small up to 50.6 GPa. After that, it was quite obvious and the (003) peak became very strong at 65.3 GPa. This might mean that the initially randomly distributed boron suboxide grains become preferably oriented due to the plastic deformation over the yield point. However, we could not observe the systematic intensity change for the boron suboxide diffraction lines at $\psi=0°$ and 90°; thus the intensity increase of the (003) peak at 65.3 GPa might be caused by the diffraction from a single crystal, which happened to be satisfied to the diffraction optics at $\psi=54.7°$.

Even under hydrostatic compression, local deviatoric stresses exist in a polycrystalline sample that result in broadening of diffraction lines.[37] The amount of broadening relative to a reference peak at ambient pressure and temperature yields a measure of the microscopic deviatoric strain distribution parallel to the diffraction vector. Fig. 7 shows the full width at half maximum (FWHM) of boron suboxide (104) and gold (111) diffraction lines vs. pressure at $\psi=54.7°$. Upon compression, the boron suboxide (104) peak broadens up to ~50 GPa and then begins to narrow. This can be also seen in Fig. 8, and may indicate that local stresses relaxed due to the plastic flow, i.e., the yield strength of the sample was exceeded. Using the ambient pressure spectrum as a reference for zero strain and assuming the grain size remain unchanged with compression, we could calculate the strain distribution in the sample under nonhydrostatic compression.[37] By multiplying by the aggregate Young's modulus, the microscopic deviatoric stresses can be determined.[37] If sufficient deviatoric stress is generated by the loading system to deform the sample plastically, then this stress represents the yield strength of the sample. However, the pressure dependence of the Young's modulus should be known to calculate the microscopic deviatoric stresses at a given pressure.

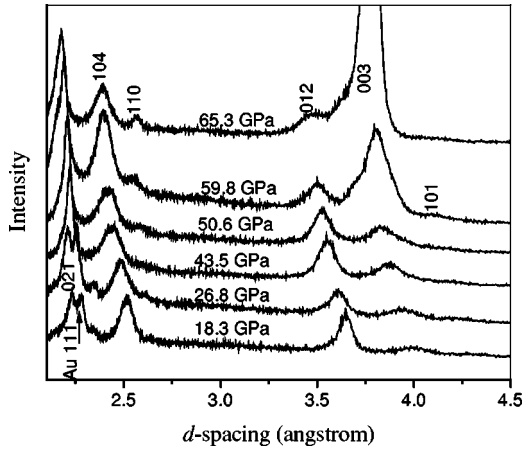

FIG. 6. Selected diffraction patterns of boron suboxide under nonhydrostatic compression taken at $\psi=54.7°$.

The aggregate Young's modulus, E, can be obtained from the bulk modulus, K, and shear modulus, G, using

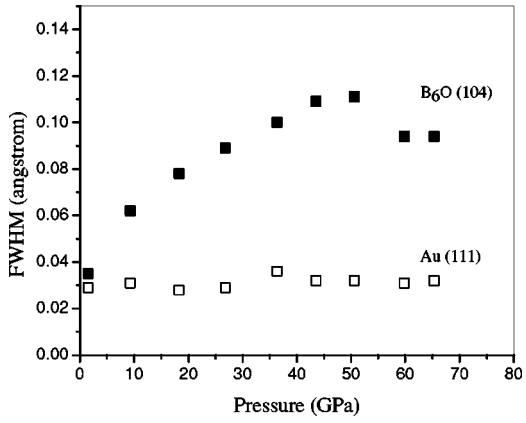

FIG. 7. The full width at half-maximum (FWHM) of B_6O (104) and Au (111) diffraction peaks vs pressure at 54.7°.

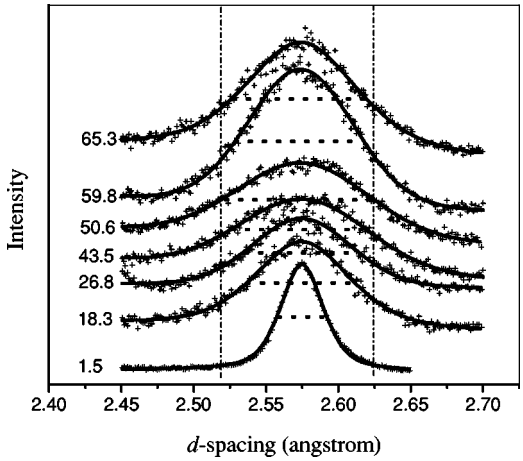

FIG. 8. (104) diffraction peak of boron suboxide at increasing pressures and ψ=54.7°. The peak position is shifted to center the bottom pattern and the intensity is rescaled. Solid curves are least-squares fit to the data (crosses). Dotted lines show the full width at half-maximum for comparison.

$$E = 9KG/(3K + G). \tag{6}$$

The bulk modulus of boron suboxide was obtained from our equation of state and the Petrak *et al.*[11] value was used for the shear modulus together with an assumed range of pressure derivatives, dG/dP, of 1.0–1.5, which are typical values for ceramics.[38] High-pressure values of K and G were computed using third order Eulerian finite strain equations. At 65 GPa, Young's modulus is estimated to be 658−740 GPa, and the shear modulus is 269−312 GPa. If we take account of the pressure dependence of Young's modulus for boron suboxide based on the above assumption, the maximal deviatoric stress calculated from the (104) peak broadening should be 26−30 GPa. Also, given the range of possible G values of 269−312 GPa at highest pressure, we have t=26−30 GPa from lattice strain theory. In addition, the calculated local deviatoric stress for gold is about 0.5 GPa, which is also close to value of the t (~0.6 GPa at ~ 40 GPa) obtained using strain theory. The above results demonstrate that the ratio of yield strength to shear modulus measured by the analysis of x-ray peak broadening is consistent with the result obtained from the strain theory, i.e., both the maximal differential stress and microscopic deviatoric stress that the sample can support under nonhydrostatic compression are equal to the yield strength once the plastic deformation is initialized.

The maximum t/G of boron suboxide [Vickers hardness 45 GPa (Ref. 1)] obtained in this study is 0.095. Using the same technique, the maximum t/G was found to be 0.037 for stishovite [Vickers hardness 33 GPa] (Ref. 17) and 0.075 for cubic silicon nitride [Vickers hardness 35−43 GPa (Ref. 36)].[35] Silicon carbide was observed to start to yield at ~14 GPa and the yield strength was measured to be 13.6 GPa by analyzing the diffraction peak broadening under nonhydrostatic compression.[39] The ratio of yield strength to shear modulus (192.5 GPa at ambient pressure[39]) of silicon carbide [Vickers hardness 25−35 GPa (Ref. 40)] is 0.071.

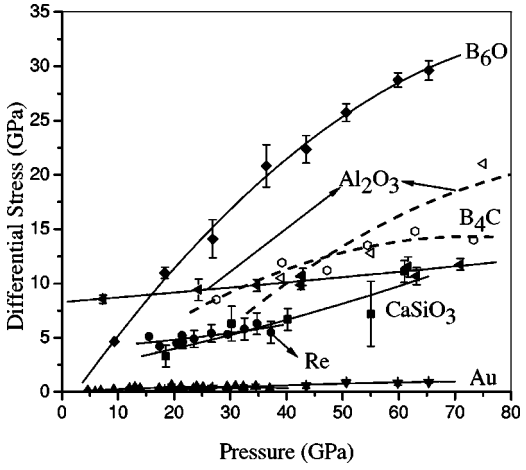

FIG. 9. Differential stress as a function of pressure. Solid symbols: static compression data (♦, B_6O from this study; ■, $CaSiO_3$ from Ref. 23; ◀, Al_2O_3 from Ref. 41; ●, Re from Ref. 18; ▼, Au from this study; and ▲, Au from Refs. 18 and 22. Open symbols: shock wave data (◁, Al_2O_3 from Ref. 43; ○, B_4C from Ref. 42). Solid lines and dashed lines: second-order polynomial fits to static compression data and shock wave data.

Except for SiO_2, it appears that the measured t/G above the yield point under nonhydrostatic compression reflects the hardness for the above strong materials. The unusual low t/G obtained for SiO_2 may be due to the stishovite-$CaCl_2$-type phase transition at around 50 GPa.[17]

Figure 9 compares differential stresses obtained for several materials from radial diffraction in the diamond-anvil cell as well as shock wave experiments. High-pressure shear moduli were obtained using third order finite strain theory and experimental values for G and dG/dP. As with B_6O, it is likely that yield has been achieved for all these materials at high pressures, so the differential stresses are equivalent to yield stresses. Also shown in the figure are data obtained from static pressure gradient measurements[41] and shock compression.[42,43] Boron suboxide is the strongest material studied to date as it supports a differential stress of 30 GPa at a confining pressure of 65 GPa. Thus, very high values of differential stress can be developed under uniaxail compression of strong, brittle solids. While this has been recognized qualitatively for some time, our results allow this to be quantified, and thus provide a useful metric for comparison of different solids and classes of solids. For examples, in strong metals such as Fe and W, differential stresses as large as 20 GPa are not developed until confining pressures of order 200 GPa are reached.[44] Indeed the differential stress supported by B_6O is about three times larger than that in rhenium metal near 30 GPa.[18] While there is limited data on high-pressure yield strengths of other strong solids, B_6O appears to be considerably stronger than other materials yet studied under static or dynamic loading. Measurements of radial pressure gradients have been used to determine maximum shear stresses in Al_2O_3 samples up to 70 GPa in the diamond cell.[41] Taking the yield or flow strength to be twice the maximum shear stress,[45] the yield strength of Al_2O_3 reaches a maximum of 12 GPa at 70 GPa,[41] which is more than a factor of 2 lower than found in B_6O. Shock wave

studies give higher values for the yield strength of Al_2O_3 but they are still well below B_6O values.[43] Other solids such as B_4C (Ref. 42) and $CaSiO_3$ (Ref. 23) also have yield strengths on the order 50% of B_6O values at high pressures. Of course, comparison of shock and static yield strengths is complicated by large differences in strain rates and also temperatures.

CONCLUSION

The presence of nonhydrostatic stress can strongly affect the EOS determination, especially for strong materials. The bulk modulus of boron suboxide derived from the nonhydrostatic compression data can vary be nearly a factor of 3 depending on the relative orientation of the diffraction vector and diamond cell stress axis. Our results demonstrate that the strength difference between the studied material and pressure standard material, as well as the angle ψ between the diffracting plane normal and stress axis, determines how the observed compression curve bias the hydrostatic curve. Using radial x-ray diffraction technique together with the lattice strain theory, we examined the behavior of boron suboxide in a diamond-anvil cell under nonhydrostatic compression up to 65.3 GPa. The hydrostatic d spacing obtained from a linear fitting to data at 0° and 90° is consistent with direct measurements at $\psi=54.7°$; thus even two measurements ($\psi=0°$ and 90°) are sufficient for accurate hydrostatic equation of state determination. The hydrostatic compression curve has been obtained at $\psi=54.7°$, which yields a bulk modulus $K_0=270\pm12$ GPa and its pressure derivative $K_0'=1.8\pm0.3$. The lower bound to the yield strength derived from the strain theory was found to be 26–30 GPa, consistent with the result obtained by the analysis of x-ray peak. This indicates that both the maximal differential stress and microscopic deviatoric stress that the sample can support under uniaxial stress are equal to the yield strength once the plastic deformation is initialized. It appears that the measured t/G above the yield point under nonhydrostatic compression reflects the hardness for the strong materials, and might be a good qualitative indicator of hardness as it reflects the contributions of both plastic and elastic deformation. Our measurements also show that B_6O is considerable stronger than others strong solids such as Al_2O_3 and $CaSiO_3$ at static high pressure.

ACKNOWLEDGMENTS

The authors thank J. Z. Hu, J. Shu, and H. K. Mao for experimental assistance, and A. Kubo for helpful discussions. This study was supported by NSF and DOE. The Carnegie-DOE Alliance Center is funded by the Department of Energy through the Stewardship Sciences Academic Alliance Program under Grant No. DE-FC03-03NA00144.

*Author to whom correspondence should be addressed; electronic mail: dhe@princeton.edu

†Current address: Dept. of Earth Sciences, National Cheng kung University, Taiwan 701, Taiwan

[1] D. W. He, Y. Zhao, L. Daemen, J. Qian, T. D. Shen, and T. W. Zerda, Appl. Phys. Lett. **81**, 643 (2002).

[2] S. Lee, D. M. Bylander, and L. Kleinman, Phys. Rev. B **45**, 3245 (1992).

[3] H. F. Rizzo, W. C. Simmons, and H. O. Bielstein, J. Electrochem. Soc. **109**, 1079 (1962).

[4] T. Lundstrom and Y. G. Andreev, Mater. Sci. Eng., A **209**, 16 (1996).

[5] T. Lundstrom, J. Solid State Chem. **133**, 88 (1997).

[6] H. F. Rizzo, W. C. Simmons, and H. O. Bielstein, J. Electrochem. Soc. **109**, 1079 (1962).

[7] H. Hubert, B. Devouard, L. A. J. Garvie, M. O'Keeffe, P. R. Buseck, W. T. Petuskey, and P. F. McMillan, Nature (London) **391**, 376 (1998).

[8] V. Srikanth, R. Roy, E. K. Graham, and D. E. Voigt, J. Am. Ceram. Soc. **74**, 3145 (1991).

[9] E. Weintraub, Trans. Am. Electrochem. Soc. **16**, 165 (1909).

[10] D. W. He, M. Akaishi, B. L. Scott, and Y. Zhao, J. Mater. Res. **17**, 284 (2002).

[11] D. R. Petrak, R. Ruh, and G. R. Atkins, Am. Ceram. Soc. Bull. **83**, 569 (1974).

[12] D. Music, U. Kreissig, V. Chirita, J. M. Schneider, and U. Helmersson, J. Appl. Phys. **93**, 940 (2003).

[13] D. M. Teter, MRS Bull. **23**, 22 (1998).

[14] J. Haines, J. M. Léger, and G. Bocquillon, Annu. Rev. Mater. Sci. **31**, 1 (2001).

[15] V. V. Brazhkin, A. G. Lyapin, Philos. Mag. A **82**, 231 (2002).

[16] R. Miletich, D. R. Allan, and W. F. Kuhs, Rev. Mineral. **41**, 447 (2000).

[17] S. R. Shieh, T. S. Duffy, and B. S. Li, Phys. Rev. Lett. **89**, 255507 (2002).

[18] T. S. Duffy, G. Shen, D. L. Heinz, J. Shu, Y. Ma, H. K. Mao, R. J. Hemley, and A. K. Singh, Phys. Rev. B **60**, 15063 (1999).

[19] A. K. Singh, H. K. Mao, R. J. Hemley, and J. Shu, Phys. Rev. Lett. **80**, 2157 (1998).

[20] A. K. Singh, J. Appl. Phys. **73**, 4278 (1993).

[21] A. K. Singh, C. Balasingh, H. K. Mao, R. J. Hemley, and J. Shu, J. Appl. Phys. **83**, 7567 (1998).

[22] T. S. Duffy, G. Shen, J. Shu, H. K. Mao, R. J. Hemley, and A. K. Singh, J. Appl. Phys. **86**, 6729 (1999).

[23] S. R. Shieh, T. S. Duffy, and G. Shen, Phys. Earth Planet. Inter. **143–44**, 93 (2004).

[24] S.-H. Shim, T. S. Duffy, and T. Kenichi, Earth Planet. Sci. Lett. **203**, 729 (2002).

[25] D. J. Weidner, L. Li, M. Davis, and J. H. Chen, Geophys. Res. Lett. **31**, L06621 (2004).

[26] M. R. Daymond and M. W. Johnson, J. Appl. Crystallogr. **34**, 263 (2001).

[27] O. L. Anderson, D. G. Isaak, and S. Yamamoto, J. Appl. Phys. **65**, 1534 (1989).

[28] I. V. Alexsandrov, A. F. Goncharov, I. N. Makarenko, A. N. Zisman, E. V. Jakovenko, and S. M. Stishov, High Press. Res. **1**, 333 (1989).

[29] I. V. Alexsandrov, A. F. Goncharov, A. N. Zisman, and S. M.

Stishov, Zh. Eksp. Teor. Fiz. **93**, 680 (1987) [Sov. Phys. JETP **66**, 384 (1987)].
[30] M. Grimsditch, E. S. Zouboulis, and A. Polian, J. Appl. Phys. **76**, 832 (1994).
[31] F. Occelli, P. Loubeyre, and R. Letoullec, Nat. Mater. **2**, 151 (2003).
[32] A. Y. Liu, M. L. Cohen, Science **245**, 841 (1989).
[33] A. Szymanski and J. M. Szymanski, *Hardness Estimation of Minerals, Rocks and Ceramics Materials* (Elsevier, Amsterdam, 1989).
[34] A. Kelly and N. H. MacMillan, *Strong Solids*, 3rd ed. (Oxford University Press, New York, 1986).
[35] B. Kiefer *et al.* (unpublished data).
[36] I. Tanaka, F. Oba, T. Sekine, E. Ito, A. Kubo, K. Tasumi, H. Adachi, and T. Yamamoto, J. Mater. Res. **17**, 731 (2002).
[37] D. J. Weidner, Y. Wang, and M. T. Vaughan, Science **266**, 419 (1994).
[38] D. G. Isaak, in *Handbook of Elastic Properties of Solids, Liquids, and Gases*, edited by M. Levy, H. Bass, R. Stern, and V. Keppens (Academic Press, San Diego, CA, 2001).
[39] J. Zhang, L. Wang, D. J. Weidner, T. Uchida, and J. Xu, Am. Mineral. **87**, 1005 (2002).
[40] G. Berg, C. Friedrich, E. Broszeit, and C. Berger, in *Handbook of Ceramic Hard Materials*, edited by R. Riedel, (Wiley-VCH, Weinheim, Germany, 2000).
[41] C. Meade and R. Jeanloz, Phys. Rev. B **42**, 2532 (1990).
[42] T. J. Vogler, W. D. Reinhart, and L. C. Chhabildas, J. Appl. Phys. **95**, 4173 (2004).
[43] W. D. Reinhart and L. C. Chhabildas, Int. J. Impact Eng. **29**, 601 (2003).
[44] R. J. Hemley, H. K. Mao, G. Shen, J. Badro, P. Gillet, M. Hanfland, and D. Hausermann, Science **276**, 1242 (1997).
[45] S. T. Weir, J. Akella, C. Ruddle, T. Goodwin, and L. Hsiung, Phys. Rev. B **58**, 11258 (1998).